JOURNAL OF APPLIED ELECTROCHEMISTRY **24** (1994) 827–834

Specificity of anodic processes in cyclic voltammetry to the type of carbon used in electrolysis of cryolite–alumina melts

S. S. DJOKIĆ*, B. E. CONWAY

Department of Chemistry, University of Ottawa, Ottawa, Ontario K1N 6N5, Canada

T. F. BELLIVEAU

Alcan International Ltd, Arvida Research and Development Centre, Jonquière, Québec G7S 4K8, Canada

Received 15 June 1993; revised 24 September 1993

Anodic processes associated with oxidation of carbon anodes used in electrolysis of cryolite–alumina melts, simulating the Hall–Héroult process, were studied by means of cyclic voltammetry in a comparative way at four graphitic carbon materials and at glassy carbon. Conditions were sought that give a current response function characteristic of diffusion-controlled oxidation of the anode by O^{2-} or oxyfluoride complex anions. Only at glassy carbon anodes are such conditions realized with a linear relation between response current in cyclic voltammetry and Al_2O_3 content in the melt. At the graphitic materials, complex mixed activation and diffusion controlled processes arise that are also relatively irreproducible from one experiment to the next, probably due to irreversible changes of the graphite surfaces. The effects of aluminium metal dissolved in the melt, to simulate practical smelter cell conditions, were also evaluated.

1. Introduction

The Hall–Héroult process, in which a melt of cryolite containing purified alumina up to about 6 wt % is electrolysed, is the principal basis for production of aluminium metal. Although the chemistry and electrochemistry of this process have been extensively studied [1–9], much remains to be understood about the reactions at the carbon anode where oxygen or oxyfluoride anions are discharged with evolution of CO_2 and some CO, COF_2 and CF_4.

In particular, when there is a depletion of oxygen-containing ions at the anode surface, onset of the so-called anode effect (AE) can arise [10, 11], a phenomenon of considerable practical importance for cell operation. It should be noted that $CF_{4(g)}$ and also $C_2F_{6(g)}$are formed *only* during AE. In industrial cells, the onset of the AE manifests itself through an immediate increase of cell voltage from values between 4.1 and 4.3 V, during normal electrolysis, to about 35–60 V [11]. Practically, the AE normally arises when the alumina content of the bath becomes too low to maintain normal operating electrolysis current-densities arising from 'alumina-depolarized' processes at the carbon anode. The AE normally arises when the alumina content declines from about 2.2 wt % to 0.5 wt % Al_2O_3, with the effect setting in commonly between 1–2% [10]. However, the reasons for this behaviour have not yet been well established. According to Jarek and Thonstad [9], conditions for onset of the AE are associated mainly with decreasing alumina concentration, increasing potential and presence of fluorocarbon surface compounds at the carbon anode. This causes a dewetting of the anode by the electrolyte and adherence of gas bubbles, a phenomenon also observed at fluorine-evolving carbon electrodes in KF–2HF melts [12].

To diminish the effect of convection on the electrode-kinetic behaviour of the electrochemical reactions, as well as to minimize disturbances at the interface due to evolution of gas, the method of fast cyclic voltammetry for study of the anodic processes in cryolite–alumina melts can be profitably used.

Although the concentration of Al_2O_3 in the melt is normally adjusted automatically in the smelter cell by means of a periodic mechanical-feed system, an *in situ* analytical probe for determination of Al_2O_3 content in molten cryolite, and thence better control of melt composition, would be particularly useful to the industry. Various attempts to use electroanalytical procedures based on the onset of diffusion control at a test-anode probe have been explored using e.g. the methods of chronoamperometry [4] and impedance spectroscopy [13, 14]. These methods are entirely satisfactory for room-temperature, aqueous-solution applications; however, they encounter substantial difficulties in a high temperature melt where the reaction of Al_2O_3 or oxygen-containing anions with carbon is a complex one, and not always diffusion controlled

---

* Present address: Sherritt Inc., Fort Saskatchewan, Alberta, T8L 3W4, Canada

under cell operating conditions. As in smelter cell operation, the AE, convection and bubble adherence effects can impair the response of such anode probes.

Calandra *et al.* [15] studied the electrode reactions that take place at carbon anodes in molten cryolite–alumina systems, with alumina content between 0.05 and 1.5 wt %. Using various sweep rates in the range 0.04–600 V s^{-1}, they observed four current peaks arising at 1.1, 1.75, 2.38 and 3.60 V. They assigned three of the four peaks to formation of CO_2, COF_2 and CF_4, respectively, while the fourth peak at 3.60 V was not discussed. Frazer and Welch [3] investigated anodic processes in cryolite–alumina melts in the concentration range 0.5–7.8 wt % Al_2O_3 and reported three current peaks at 1.1, 1.7 and 2.2 V positive to the aluminium potential. They attributed the peaks at 1.1 and 1.7 V to CO and CO_2 formation, while the peak at 2.2 V was not discussed. Jarek and Thonstad [8, 9] performed very fast cyclic voltammetry measurements on graphite in molten cryolite with alumina additions in the range 0.25–2 wt % and 0.25–5 wt %. The five current peaks they observed for a sweep rate of 10 V s^{-1} and an alumina content of 0.5 wt %, arose at 1.1, 1.98, 2.57, 3.24 and 4.73 V. They observed a corresponding reduction peak, conjugate to the first peak at about 1.1 V, in the cathodic branch but the process was not reversible [8]. They attributed these peaks to absorption/desorption of discharged oxygen species, forming carbon–oxygen surface compounds. The second, third, fourth and fifth peaks [9] they attributed to highly irreversible reactions involving the formation of CO_2, COF_2, CF_4 and F_2, respectively. They found the dependence of the potential of the first peak on alumina concentration up to 5% to be almost uniform. On the other hand, the potential of the first peak increased significantly with increasing sweep rate [8]; for such behaviour, however, the calculated reaction charge decreased, while for sweep rates above 100 V s^{-1}, the charge attained a constant level.

The anodic current peak depended linearly on the alumina concentration but only up to an alumina content in the melt of 1%. With an increase of alumina concentration beyond this value, up to about 5%, they observed no further significant change in the first peak current. They examined this in terms of the possibility that the supposed adsorption reaction at carbon,

$$(O^{2-})_{bath} \rightleftharpoons (O^{2-})_{ads}, \qquad (1)$$

reaches saturation at around 1% Al_2O_3 in the melt.

The location, on the potential scale, of the peak potential depends, according to Jarek and Thonstad, on the alumina concentration [9]. In this way, it was found, for the second and third peaks, that a linear relationship exists between the potential and alumina concentration over the concentration range 0.25 to 2%. However, the potentials of the fourth and fifth peaks were independent of the alumina concentration within the range 0.25 to 1% Al_2O_3.

Table 1. Characteristics of glassy carbon and graphites used as the anode materials

Carbon material	*Apparent density*	*Shore hardness*	*Ash content*	*Porosity*
Glassy carbon	1.50	120	0.04%	0%
Graphite 208	1.68	34	< 2 p.p.m.	23%
Graphite 238	1.60	17	< 2 p.p.m.	28%
EPB	1.68	–	0.12%	–
ATJ	1.74	–	0.008%	–

Also, it was shown that a linear relationship exists between the square root of the peak currents (for the second and third peaks) and the alumina concentration over the concentration range 0.25 to 2% wt %, i.e. the processes associated with these peaks are likely to be mass-transfer controlled under these conditions.

The aims of the present work were as follows: (a) to examine the response-signal behaviour in cyclic voltammetry at various kinds of carbon indicator (working) anodes in order to identify one or more materials at which the current response is mainly diffusion controlled and hence proportional to Al_2O_3 concentration; and (b) to examine the d.c. Tafel polarization behaviour of several carbon anode materials with respect to the kinetics of carbon oxidation by O^{2-} or other oxygen-containing anions of the cryolite melt in order to identify the relative roles of diffusion and activation control in the complex processes that are involved in carbon oxidation in cryolite containing dissolved Al_2O_3.

2. Experimental details

2.1. *General*

In the present work, the new aspects of the study of the reaction of alumina at carbon anodes involved investigation of the effect of *type* of carbon used as the anode material by means of (i) the examination of several graphitic anode materials, distinguished by the following commercial designations: 208 and 238 (products of Carbone Lorraine), EPB and ATJ (products of Union Carbide); (ii) a comparative examination of glassy carbon (Carbone Lorraine product) behaviour in relation to that of the graphites (characteristics of graphitic materials and of glassy carbon, according to producers, are presented in Table 1); and (iii) an examination of the relation of cyclic voltammetry current response to anodic Tafel polarization behaviour and the role of the diffusion of oxide or oxyfluoride anion species to the electrode.

2.2. *Procedures and experimental conditions*

Experiments were performed in an open graphite crucible exposed to the atmosphere. A bath containing 650 g Na_3AlF_6 (product of Bayer), 30 g Baker reagent grade CaF_2, with additions of Al_2O_3 from 0 to 50 g (0–6.85%) was used for investigating the anodic reactions.

The anodes consisted of carbon rods, 3.08 mm in diameter, press fitted into boron nitride sheaths, 2.5 cm in diameter, to provide mechanical stability. Before insertion into the sheaths, the graphite rods received a pyrolytic boron nitride coating 0.12 mm thick. The glassy carbon rods could not be treated similarly due to their lack of porosity. The boron nitride coatings permitted the anodes to present a geometrically circular surface to the working solution by providing a barrier along the sides of the anodes. The geometrical surface area of the working electrode in contact with the molten electrolyte was about 0.075 cm^2. The counter electrode (a graphite rod having a diameter of 1 cm) was immersed to a depth of about 2 cm in the melt. An aluminium metal (molten) reference electrode was housed in a separate boron nitride compartment provided with a small hole giving access to the melt. The contact with the aluminium reference electrode was by means of a tungsten wire on the surface of which aluminium had previously been plated.

The experiments were performed at a temperature of 1000 ± 2° C.

The cyclic voltammetry experiments were carried out using a universal potentiostat/galvanostat, PAR model 273, controlled via a personal computer executing M270 PAR electrochemical software. The sweep rate in the cyclic voltammetry experiments was varied from 1 to 80 V s^{-1} in the potential ranges 0.4 to 2.25 V and 0.4 to 4.0 V, depending on requirements. Before each cyclic potential scan, the system was conditioned at 0.4 V for 15 s, an empirical procedure found to improve reproducibility of results. Also, before each series of experiments, the uncompensated ohmic drop was measured with the same equipment, using positive feedback. Peak currents were measured from the baseline of the charging current but, with the high temperature system studied, this baseline was not as well defined as commonly is the case in aqueous-solution studies [16]. Significant background currents unavoidably arise and impair the accuracy and reproducibility of the cyclic voltammentry results obtainable at carbon electrodes in the melt at high temperature. It is probable that the background current arises on account of oxidation of low oxidation state aluminium species plus solvated electrons present (see below) in the melt, due to significant dissolution of aluminium metal in the cryolite.

The electrochemical measurements were carried out under two separate conditions. First, the anodic processes on the glassy-carbon electrode material were investigated in cryolite–alumina melts of various compositions without addition of aluminium metal. In the second series of experiments, anodic processes on a series of other carbon electrode materials, including glassy carbon, were investigated in the same series of cryolite–alumina melts but in which aluminium metal (approximately 22 ± 2 g) had been added to 650 g of cryolite electrolyte.

The examination of melts containing dissolved aluminium metal is of practical importance since electrochemical aluminium smelter baths unavoidably contain small, but significant concentrations of dissolved aluminium [10].

3. Results and discussion

Before evaluating information from the recorded response functions for the system investigated by means of cyclic voltammetry, it was necessary to determine, and compensate for, the effects of 'uncompensated resistance' (iR-drop effect). The results showed that the uncompensated resistance, R_u, had typical values between 0.8 and 1.5 Ω which depended on the alumina content of the melt as well as on the type of carbon used. In dealing with the results arising from the experiments conducted in this work, as referred to earlier, the effect of uncompensated resistance was taken into consideration in the recording and/or analysis of results from all experiments.

3.1. *Behaviour at the glassy carbon electrode with no added aluminium*

The results of experiments with no added aluminium metal in the bath showed behaviour substantially different from that of the corresponding system containing added aluminium.

First, the open circuit potential in these experiments was unsteady, decreasing with increasing alumina concentration in the melt. The most frequently observed values of the open-circuit potential were about 0.8 V when the melt did not contain any alumina and about 0.4 V when the bath contained 40 g alumina (5.56 wt %).

Secondly, the results were not reproducible in a desirable way.

A typical cyclic voltammogram is shown in Fig. 1. Four anodic peaks are distinguishable, arising at potentials of 1.2, 2.1, 2.8 and 3.6 V (cf. [15]), approximately. For the present purpose we investigated behaviour over the potential range 0.4 to 2.25 V. The first peak can be related to evolution of carbon–oxygen compounds, CO and/or CO$_2$, because the peak height was dependent on the concentration of alumina in the melt.

It is to be noted that the current responses in the positive-going and negative-going sweeps are not like those for underpotential deposition processes, e.g. of H or OH/H at platinum where such curves correspond to anodic and cathodic processes, respectively. Here both directions of the curves represent faradaic current responses that are always in the *anodic* direction but are in various ways influenced by irreversibility in the anodic reactions that take place in the directions of increasing and decreasing positive potentials; probably owing to progressive changes in the state of the surface of the carbon during the first positive-going sweep. Thus, currents on the negative-going sweeps are always substantially less than

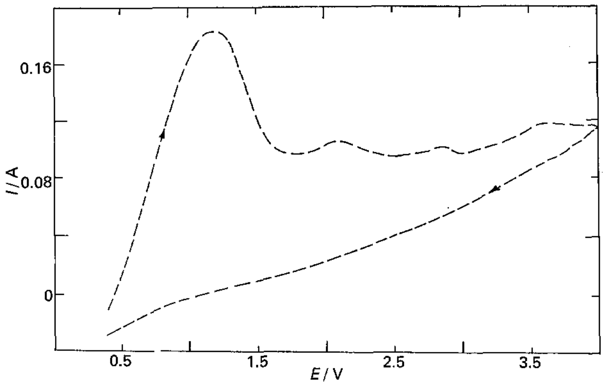

Fig. 1. Cyclic voltammogram for anodic oxidation processes at the glassy carbon electrode with no aluminium metal present ($s = 80\,V\,s^{-1}$, 30 g Al_2O_3).

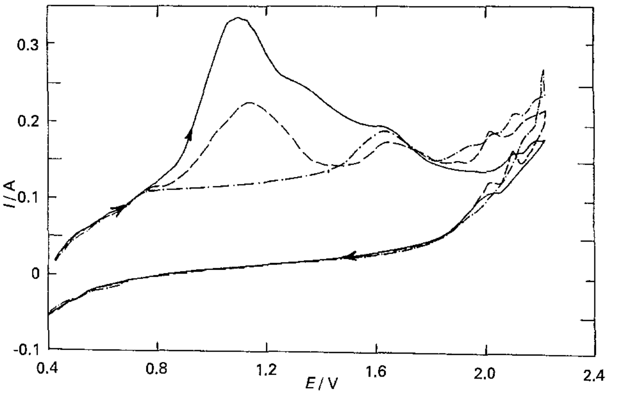

Fig. 3. Cyclic voltammogram for anodic oxidation process at the graphite ATJ material ($s = 10\,V\,s^{-1}$, 10 g Al_2O_3), (——) first, (— — —) second and (—· — ·) third sweep).

those at corresponding potentials on the positive-going sweep, i.e. by much more than could be accounted for by the opposite direction of the double-layer charging current.

3.2. *Behaviour at various carbon electrodes with added aluminium metal in the melt*

Metallic aluminium dissolves significantly in molten cryolite, although the nature of the dissolved species is still uncertain [10, 11]. Additionally, cryolite melts wet graphite surfaces much better when dissolved aluminium is present. It seems that the differences in wetting (or corresponding differences of surface tension and contact angle of bubbles) lead to higher peak currents on account of the effective anode surface in contact with the melt becoming substantially larger, due to the better wetting.

A typical cyclic voltammogram for the cryolite–alumina melt, using graphite ATJ as the anode is shown in Fig. 2. This voltammogram displays four distinguishable anodic current peaks arising at approximately 1.1, 1.95, 2.45 and 3.3 V. The first peak was not reproducible, and it is to be noted that sometimes this peak current was quite high as indicated in Fig. 3. This peak has been observed also by other workers [3, 8, 9, 15]. Recently, Jarek and Thonstad [8] reported a study devoted to the behaviour of the first peak and found that the current for this peak was reproducible and may be connected with electrosorption of oxygen, leading to formation of a carbon–oxygen surface compound. Irreproducibility of this peak in our work, contrary to the observations of Jarek and Thonstad, can be explained by the different conditions used in our experiments: the use of an open crucible, exposed to atmospheric air, to simulate the situation in real industrial cells.

The second, third and fourth peak current values were, however, satisfactorily reproducible. To observe such behaviour, it was necessary, however, to restrict the voltammetric experiment to just one cycle. When experiments were carried out over more than one cycle, the results became significantly more irreproducible, as exemplified in Fig. 4. This irregularity could be related to possible electrosorption of oxygen-containing species during the first cycle. Due to deactivation of the electrode surface, the second and any successive sweeps show much lower current.

Importantly, it was found that the shape and peak current values of voltammograms depended on the kind of graphite used as the working electrode, as can clearly be seen by comparing the results shown in Figs 2 and 5–8. It is important to note that no *cathodic* currents arise in the negative-going

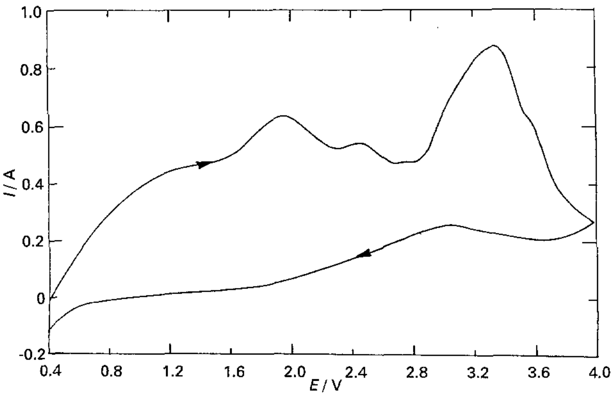

Fig. 2. Cyclic voltammogram for anodic oxidation process at the graphite ATJ material ($s = 80\,V\,s^{-1}$, 30 g Al_2O_3).

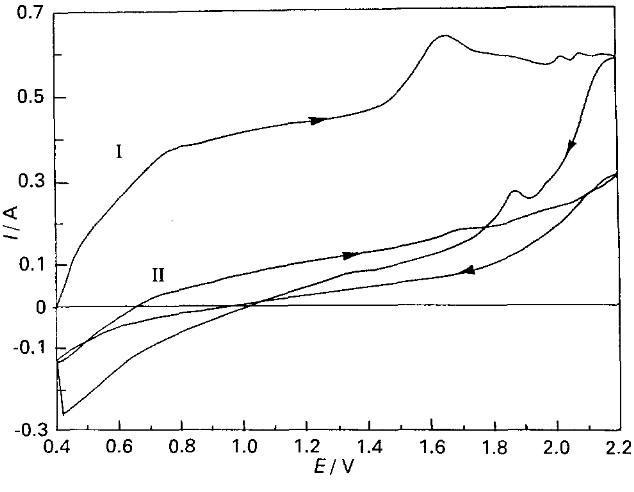

Fig. 4. Cyclic voltammogram for anodic oxidation process at the graphite EPB ($s = 80\,V\,s^{-1}$, 30 g Al_2O_3), (I) first cycle, (II) second cycle).

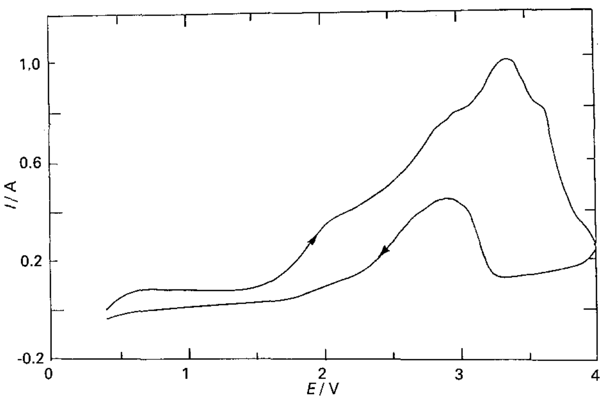

Fig. 5. Cyclic voltammogram for anodic oxidation process at glassy carbon ($s = 80\,V\,s^{-1}$, 30 g Al_2O_3).

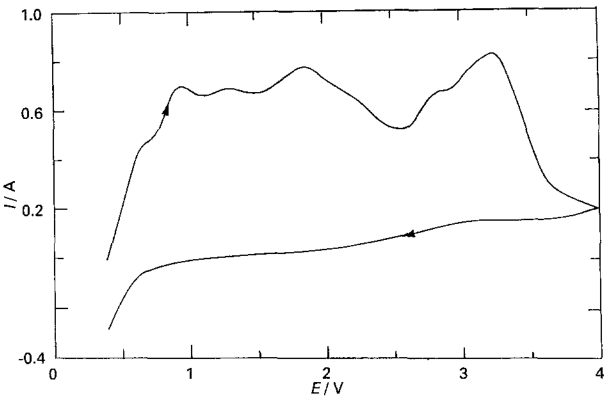

Fig. 7. Cyclic voltammogram for anodic oxidation process at the graphite 238 material ($s = 80\,V\,s^{-1}$, 10 g Al_2O_3).

directions of the sweeps in the voltammograms. This behaviour therefore indicates a high degree of irreversibility of the processes involved, unlike, for example, underpotential deposition or metal surface oxidation. In the case of glassy carbon, on the negative going sweep curves of the voltammogram, between 2 and 3.2 V, relatively high anodic currents were recorded (Fig. 5). The sharp decrease in current at 3.5 V and a subsequent absence of current flow on the reverse sweep between 4 and 3.2 V clearly indicate the occurrence of an 'anode effect'. Around 3.2 V, the anode comes out of the 'anode effect' permitting current to flow again. On the other hand, Fig. 1 does not show any anode effect on a glassy carbon anode in the melt with no added aluminium metal. Figures 2 and 7 show an anode effect on the reverse sweeps for graphites ATJ and 238, but Figures 6 and 8 for graphites 208 and EPB do not. The reasons for these inconsistencies are not clear, although they are somehow connected with the nature of the carbon anode used in the experiments. Larger currents recorded at the glassy carbon electrode in the case of experiments with aluminium metal present in the melt (Fig. 5) than in the case of experiments with no added aluminium, could be explained by the wetting properties of the melt. As mentioned earlier, cryolite melts wet electrode surfaces much better when dissolved aluminium is present [11], leading to higher currents on account of an increase of the effective anode surface in contact with the melt.

Further discussion of the cyclic voltammetry results will be restricted to the behaviour of the main, second, peak (1.95 V) at the several kinds of carbon materials investigated.

According to the results obtained, Table 2 summarizes the characteristic behaviour of the response functions in cyclic voltammetry at various carbon materials used as anodes in the Na_3AlF_6–Al_2O_3 melts.

Although, with increase of square root of sweep rate, the peak current increases for all the kinds of carbon investigated, these dependences, with the exception of that at glassy carbon, did not follow the linear relationship expected for a diffusion-controlled process. Correspondingly, the shapes of the Tafel plots do not follow that expected for a diffusion-controlled reaction. Typical results are presented in Fig. 9, for the graphite ATJ. Similar results were obtained on the other graphite materials used, but the behaviour of glassy carbon was importantly different.

In the latter case, the dependence of peak current on square root of sweep rate is *linear* over all the range of concentrations of alumina employed. This dependence indicates, of course, that the process *is* diffusion controlled under these conditions.

This conclusion is confirmed by the results in Fig. 10 where the anodic Tafel plot for this electrode material is shown and exhibits a clear approach to a limiting current of about $9\,mA\,cm^{-2}$, corresponding to diffusion control; agitation of the melt increases this current appreciably but in an irregular way.

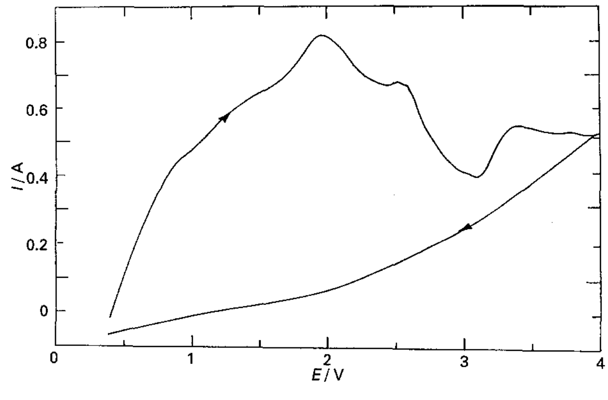

Fig. 6. Cyclic voltammogram for anodic oxidation process at the graphite 208 material ($s = 80\,V\,s^{-1}$, 40 g Al_2O_3).

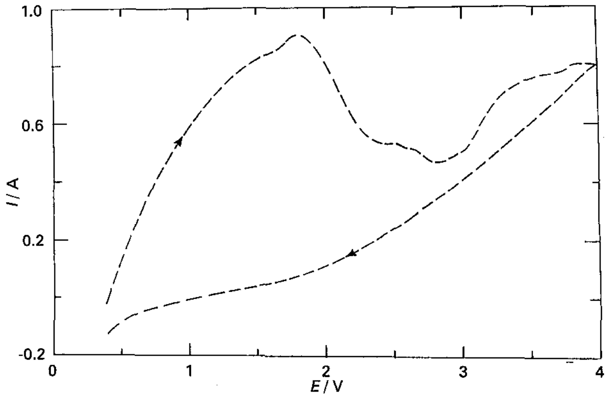

Fig. 8. Cyclic voltammogram for anodic oxidation processes at the graphite EPB material ($s = 80\,V\,s^{-1}$, 30 g Al_2O_3).

Table 2. Characteristic behaviour of response functions in cyclic voltammetry at carbon materials as anodes in Na_3AlF_6/Al_2O_3

Carbon material	$I_p/s^{1/2}$	E_p/s	I_p/Al_2O_3 *conc.*
Glassy carbon	These dependences were linear for all concentrations of Al_2O_3, and show an increase of I_p with increase of s	E_p increases with s increase	I_p increases in an approximately linear way with Al_2O_3 content increase up to 4%
Graphite 208	I_p increases with increase of s, but not in a linear way, and results are not reproducible from day to day	E_p increases with s increase	Not smooth dependence. Sometimes I_p increases with Al_2O_3 concentration, sometimes it is almost independent of Al_2O_3 concentration
Graphite 238	I_p increases with increase of s	E_p increases with increase of s	I_p increases with Al_2O_3 concentration increase, but not in a linear way
EPB	I_p increases with increase of s in no linear way	E_p increases with increase of s	I_p is almost independent of Al_2O_3 concentration
ATJ	I_p increases with increase of s in no linear way	E_p increases with increase of s	I_p increases with Al_2O_3 concentration increase

Also, the irregularities seen in Figs 9 and 10 arise due to formation and detachment of CO_2 bubbles from the carbon surface.

The potential of the second peak increases with increasing sweep rate, as for an irreversible process, for all investigated concentrations of Al_2O_3 and for each of the types of carbon investigated (see above). On the other hand, no systematic or significant trend of the dependence of peak potentials on the alumina concentration for all applied sweep rates and for all the kinds of carbon used, could be observed.

The relationships of the peak current values to alumina content in the melt are found to be strongly determined by the kind of carbon used as the electrode. Although, in some cases, an increase of peak current can be related to an increase of Al_2O_3 concentration (graphites 208, 238, EPB, ATJ), these results were not reproducible, neither was there any observable or reproducible linear relationship between current maxima values and Al_2O_3 concentration.

On glassy carbon electrodes, on the other hand, the dependence of the peak current values on alumina content in the range 1.45–4.23 wt% Al_2O_3 *was* observed to follow a more satisfactory linear relationship, as shown in Fig. 11. According to the I_p versus $s^{1/2}$ plot (Table 2), or the Tafel plot (Fig. 10), such results are to be expected for the glassy carbon electrode.

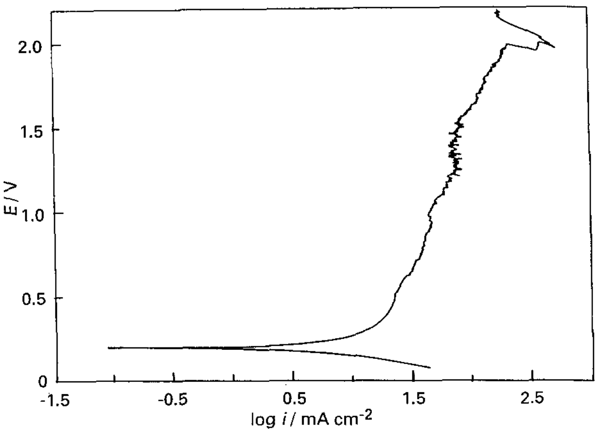

Fig. 9. Anodic Tafel plot for graphite ATJ material in a melt containing 40 g Al_2O_3 per 650 g cryolite.

It seems that the nature of the carbon electrodes used has a strong effect on the character of the anodic processes as investigated in the cyclic voltammetry experiments. According to the present results, the anodic processes are diffusion controlled under the conditions investigated *only* at the glassy carbon surfaces. On the electrodes prepared from the other graphitic carbon materials, the limiting factor is probably the process of adsorption and/or reaction of oxygen-containing electroactive species at the electrode surface [17].

Such behaviour is probably related to the structure, density, chemical bonding and other properties of the graphitic carbon electrode materials investigated.

3.3 *Discussion of mechanistic aspects of carbon oxidation*

The anodic process of reaction of alumina at carbon

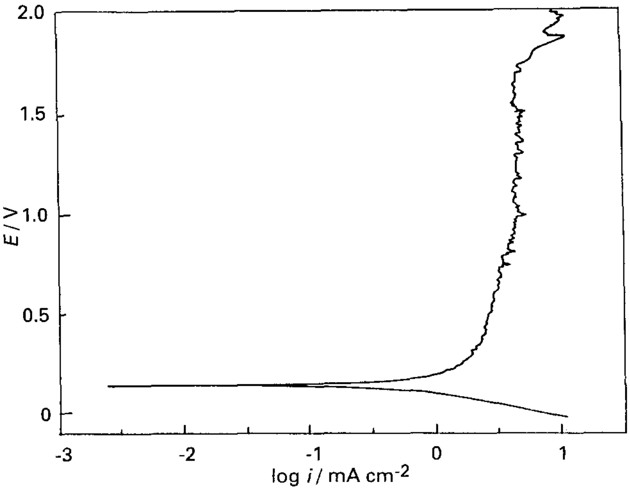

Fig. 10. Tafel plot for glassy carbon, in a melt containing 30 g Al_2O_3 per 650 g cryolite.

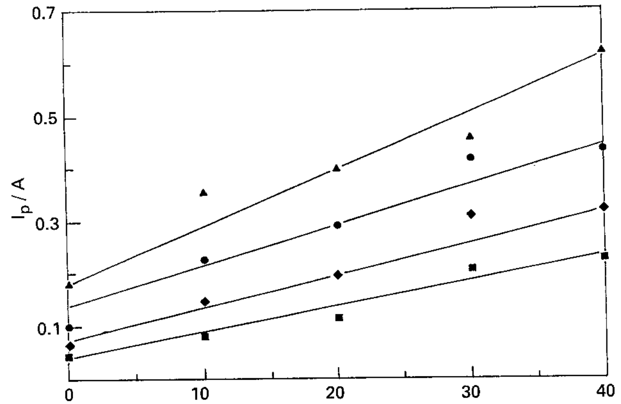

Fig. 11. Dependence of peak current in cyclic voltammetry at glassy carbon on alumina content in the melt for different sweep rates, *s* (working electrode, glassy carbon; sweep potential range from 0.4 to 2.25 V against aluminium reference electrode in the melt): (▲) 60, (●) 40, (◆) 20 and (■) 10 V s^{-1}.

involves the 'depolarized' discharge of O^{2-}, or other negatively charged oxyanion species, through reaction with the consumable carbon anode according to the following possible overall cell reactions [9, 15]:

$$Al_2O_3 + 3C \rightleftharpoons 2Al + 3CO \qquad (2)$$

$$E^0 = 1.024\,V \text{ at } 1010°C$$

$$\tfrac{2}{3}Al_2O_3 + C \rightleftharpoons \tfrac{4}{3}Al + CO_2 \qquad (3)$$

$$E^0 = 1.16\,V \text{ at } 1020°C,$$

$$\tfrac{2}{3}Na_3AlF_6 + \tfrac{1}{3}Al_2O_3 + C \rightleftharpoons COF_2 + 2NaF + \tfrac{4}{3}Al$$

$$E^0 = 1.80\,V \text{ at } 1020°C, \qquad (4)$$

$$\tfrac{4}{3}Na_3AlF_6 + C \rightleftharpoons CF_4 + 4NaF + \tfrac{4}{3}Al \qquad (5)$$

$$E^0 = 2.50\,V \text{ at } 1020°C,$$

and

$$\tfrac{2}{3}Na_3AlF_6 \rightleftharpoons \tfrac{2}{3}Al + 2NaF + F_2 \qquad (6)$$

$$E^0 = 4.42\,V \text{ at } 1020°C.$$

According to the existing data in the literature, there are disagreements concerning the significance of the second peak. Frazer and Welch [3] attributed the peak (at 1.74 V) to CO_2 formation and evolution. Calandra *et al.* [15] assigned the corresponding peak at 1.75 V to COF_2 formation. Recently, Jarek and Thonstad [9] attributed the peak at 1.98 V to evolution of CO_2, as mentioned earlier. However, most of these assignments must remain speculative in the absence of controlled-potential gas analysis experiments.

We believe that the second peak should be attributed to formation and evolution of COF_2. The reasons for this conclusion are as follows:

(i) Regardless of the investigation, in this present work using several kinds of carbon as the working electrode, it is clearly found that the potential of the second peak has a value between 1.5 and 1.8 V (depending on the sweep rate, as well as on the kind of carbon used), with the exception of glassy carbon, where corresponding values for the potential of the second peak were between 1.6 and 2.0 V. This sequence seems to be quite consistent with the values of the potentials, E^0, given for Reaction 4, notwithstanding some indications of irreversibility of the process involved.

(ii) This peak was also both observable and reproducible in the case when cyclic voltammetry was applied at glassy carbon in the cryolite melt alone, without the presence of any aluminium.

(iii) Finally, if the process involves only CO_2 formation and evolution, the relationship of peak current I_p against alumina content, or $I_p^{1/2}$ against alumina content should be linear. However, our results do not show such smooth dependence of I_p or $I_p^{1/2}$ on alumina concentration. Although, in some cases, an increase of peak current with alumina concentration was actually observed, the experimental values of the peak current were substantially less than those that could be calculated, based on the diffusion coefficient and a given value of Al_2O_3 concentration. For the above and other reasons, it seems more reasonable to accept that this process is related mainly to evolution of COF_2 rather than CO_2.

3.4. *Dependence of behaviour on type of anode carbon*

The present results show clearly and importantly that the nature of the investigated process depends on the *kind* of carbon used. It is to be noted that the carbon oxidation process, in the case of glassy carbon, is probably under almost complete diffusion control. However, the results obtained with other kinds of carbon indicate that the carbon oxidation process is probably under mixed activation and diffusion control, so that an explicit electroanalytically significant response current behaviour is then difficult to observe.

Although it remains to be proven that formation of COF_2 is the primary product associated with the second peak, which is a difficult problem [18] to be solved, this process can be interpreted, according to Calandra *et al.* [15], in the following way. Fluoride ions are discharged on the 'C_xO' intermediates covering the electrode surface.

$$xC + O^{2-}_{(ad)} \rightleftharpoons C_xO^{-}_{(ad)} + e^- \qquad (7)$$

$$C_xO^{-}_{(ad)} \rightleftharpoons C_xO_{(ad)} + e^- \qquad (8)$$

According to the overall Reaction 4, the formation of COF_2, involves the following steps:

$$C_xO_{(ad)} + F^- \rightleftharpoons C_xOF_{(ad)} + e^- \qquad (9)$$

$$C_xOF_{(ad)} + F^- \rightleftharpoons COF_{2(ad)} + (x-1)C + e^- \qquad (10)$$

$$COF_{2(ad)} \rightleftharpoons COF_{2(gas)} \qquad (11)$$

On the other hand, although the formation of $COF_{2(g)}$ theoretically explains the second peak reasonably well, it should be noted that $COF_{2(g)}$ has never been found in the industrial cell gas. This may be because the industrial cells seldom attain the necessary anode overvoltage of 0.64 V (=1.80–1.16 V) required for appreciable production of

$COF_{2(g)}$. If COF_2 were produced under these conditions, it would quickly hydrolyse with moisture in the air to $CO_{2(g)}$ and $HF_{(g)}$.

According to the results obtained, it is evident that the systems investigated are very complicated, and their behaviour depends not only on the alumina content but also materially and importantly on the *type* of carbon used as the working electrode, as well as on some other, different factors such as the presence or absence of aluminium metal [11], as found also in the present work.

From the results obtained, it is evident that the type of carbon used as the anode indicator electrode for the required electroanalytical response-current signal, determines, in an important way, both the extent to which the response current is determined only by a diffusion-controlled process or by a mixed one involving activation control, resulting in irreproducibility of results. Only for conditions where the process is purely, or more or less, fully diffusion controlled, as found in the present work for glassy carbon, is a satisfactory electroanalytical procedure realizable. However (cf. [13], dealing with an application of impedance evaluation at various concentrations), in certain cases where an activation-controlled current has a well defined relation to bulk reactant concentration (i.e. for a process with a well defined reaction order, cf. [16]), the response current, related to concentration, can have electroanalytical significance. A complication, found in the present work, is that the background current behaviour depends (a) on the carbon material, so a material-dependent modification of the expected ideal current response to alumina concentration is an additional but unavoidable complication, and (b) on the presence or otherwise of aluminium metal in the melt which can provide an additional anodic partial current at the carbon.

Our significant practical conclusion from the present work is, however, that *glassy carbon* indicator electrodes are, by far, the most satisfactory for establishing a meaningful electroanalytical response current, i.e. one almost linear in the analyte concentration. This means, in terms of electrode kinetics, that the heterogeneous processes of carbon oxidation are kinetically most facile at this material, perhaps due its *non*graphitic nature. This corresponds to the observation of approach to limiting currents in the Tafel plots (Figs 9, 10) as current density is increased, and to the increase of such currents when the melt suffers stirring or self-disturbance due to bubble formation and detachment.

Acknowledgements

Thanks are due to the Government of Ontario for matching support of this project and to Dr. F. Kimmerle of Alcan International for useful discussions during the research.

References

[1] J. Thonstad, *Electrochim. Acta* **15** (1970) 1569.
[2] *Idem, ibid.* **15** (1970) 1581.
[3] E. J. Frazer and B. J. Welch, *Proc. Austral. Inst. Min. and Met.* **260** (1976) 17.
[4] D. Damianacos, F. Lantelme and M. Chemla, *J. Chim. Phys.* **76** (1979) 391.
[5] A. J. Calandra, C. E. Castellano and C. M. Ferro, *Electrochim. Acta* **30** (1985) 1149.
[6] F. Lantelme, D. Damianacos and M. Chemla, *J. Electrochem. Soc.* **127** (1980) 498.
[7] E. W. Dewing and E. T. van der Kouwe, *ibid.* **124** (1977) 58.
[8] S. Jarek and J. Thonstad, *ibid.* **134** (1987) 856.
[9] *Idem, Electrochim. Acta* **32** (1987) 743.
[10] K. Grjotheim, C. Krohn, M. Malinovský, K. Matiašovský and J. Thonstad, 'Aluminium Electrolysis: Fundamentals of the Hall–Héroult Process', 2nd edn, Aluminium Verlag, Düsseldorf (1982).
[11] I. A. Troicky and V. A. Zheleznov, 'Metallurgiya Alyuminiya', Izd. Metallurgiya, Moscow (1984) (in Russian).
[12] L. Bai and B. E. Conway, *J. Appl. Electrochem.* **20** (1990) 925.
[13] G. S. Picard, E. C. Prat, Y. J. Bertaud and M. J. Leroy, 'Light Metals' (edited by R. D. Zabreznik), Metall. Soc. America, Warrendale (1987) pp. 507–17. (1987) p. 507.
[14] G. Picard, Y. Bertaud and E. Prat, *US Patent 4 935 107* (1990).
[15] A. J. Calandra, C. E. Castellano and C. M. Ferro, *Electrochim. Acta* **24** (1979) 425.
[16] A. J. Bard and L. A. Faulkner, 'Electrochemical Methods', John Wiley and Sons, New York (1980).
[17] J. Thonstad, *Electrochim. Acta* **13** (1968) 449.
[18] J. C. Amphlett, J. R. Dacy and G. O. Pritchard, *J. Phys. Chem.* **75** (1971) 3024.